BIOCHEMISTRY
including biophysical chemistry & molecular biology

Article

pubs.acs.org/biochemistry

The Crystal Structure of Human Endoplasmic Reticulum Aminopeptidase 2 Reveals the Atomic Basis for Distinct Roles in Antigen Processing

James R. Birtley,[†] Emmanuel Saridakis,[†] Efstratios Stratikos,*[,‡] and Irene M. Mavridis*[,†]

[†]Structural and Supramolecular Chemistry Laboratory, Institute of Physical Chemistry, National Center for Scientific Research Demokritos, Aghia Paraskevi 15310, Athens, Greece

[‡]Protein Chemistry Laboratory, IRRP, National Center for Scientific Research Demokritos, Aghia Paraskevi 15310, Athens, Greece

Supporting Information

ABSTRACT: Endoplasmic reticulum aminopeptidases ERAP1 and ERAP2 cooperate to trim a vast variety of antigenic peptide precursors to generate mature epitopes for binding to major histocompatibility class I molecules. We report here the first structure of ERAP2 determined at 3.08 Å by X-ray crystallography. On the basis of residual electron density, a lysine residue has been modeled in the active site of the enzyme; thus, the structure corresponds to an enzyme−product complex. The overall domain organization is highly similar to that of the recently determined structure of ERAP1 in its closed conformation. A large internal cavity adjacent to the catalytic site can accommodate large peptide substrates. The ERAP2 structure provides a structural explanation for the different peptide N-terminal specificities between ERAP1 and ERAP2 and suggests that such differences extend throughout the whole peptide sequence. A noncrystallographic dimer observed may constitute a model for a proposed ERAP1−ERAP2 heterodimer. Overall, the structure helps explain how two homologous aminopeptidases cooperate to process a large variety of sequences, a key property of their biological role.

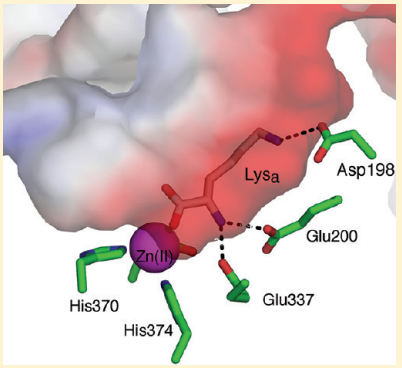

The intracellular generation of small peptide fragments that are subsequently presented on the cell surface by specialized receptors of the major histocompatibility class I family (MHCI) is central to the cytotoxic T-cell response. MHCI receptors have stringent requirements in peptide length and usually bind and present peptides that are 8−10 amino acids long. These peptides are generated inside the cell from the degradation of intracellular or endocytosed proteins through the ubiquitin−proteasome pathway.[1,2] The proteasomal products are usually larger than the mature antigenic peptide, having additional amino acids at their N-termini that have to be removed so that the antigenic peptide generated is of the appropriate length to bind onto MHCI receptors.[3] This is achieved inside the endoplasmic reticulum (ER) by specialized ER-resident aminopeptidases.[4,5]

Two homologous ER aminopeptidases have been identified to date that trim antigenic peptide precursors so that they can bind to MHCI molecules. The best characterized of the two, ERAP1, has been shown to be required for the generation of many antigenic epitopes both in vitro and inside cells.[6,7] ERAP1 knockout mice were found to be deficient in the generation of many epitopes but also present an altered peptide repertoire on their surface, suggesting that ERAP1 epitope-mediated trimming can influence immunodominance.[8−10] Furthermore, ERAP1 is specialized for trimming relatively large peptides (10−16 amino acids long) while sparing short ones, a property that is consistent with its biological role in preparing peptides for MHCI binding.[11,12] Finally, ERAP1 can also destroy several antigenic epitopes by trimming them to lengths inappropriate for MHCI binding.[6] This dual function of ERAP1 has led to its characterization as an antigenic peptide editor.[10,13]

Given the enormous number of protein sequences that are sampled by the proteasomal antigen generation and processing pathway, ER-resident aminopeptidases are expected to process efficiently a very large number of different peptide sequences. ERAP1, however, has been shown to have preferences for peptide−substrate sequences, a property that may at least partially explain antigenic peptide selection but opens questions regarding the processing of many epitopes that are poorly trimmed by ERAP1.[14] In an effort to address this, researchers identified ERAP2, a highly homologous aminopeptidase that is colocalized with ERAP1 but presents distinct specificity for the N-terminal residue of the peptide substrate.[15,16] ERAP2 was shown to be able to complement ERAP1 activity by removing N-terminal amino acids from epitope precursor sequences that ERAP1 processed poorly. Furthermore, ERAP2 was found to physically associate with ERAP1, forming a heterodimer.[15] This proposed ERAP1−ERAP2 complex would be expected to be more efficient in

Received: August 7, 2011
Revised: November 22, 2011
Published: November 22, 2011

dealing with the large number of sequences that need to be processed compared to a single enzyme.

The importance of antigen processing by ERAP1 and ERAP2 has been recently highlighted by several population-wide genetic studies that have linked single coding nucleotide polymorphisms (SNPs) found in those two enzymes with several human diseases.[17] Specifically, an ERAP1−ERAP2 haplotype has been linked with the chronic inflammatory disease Ankylosing Spondylitis, a disease with a strong hereditary autoimmune component.[18] Recent analysis of ERAP1 SNPs suggested that this link may be mediated through effects on the antigenic processing properties of the enzyme.[19] Furthermore, ERAP1−ERAP2 haplotypes have been linked with resistance to HIV infection, presumably through altered processing of HIV epitopes.[20−22] A specific ERAP2 polymorphism has been linked with predisposition to preeclampsia.[23] Finally, ERAP1 and ERAP2 levels have been found to be either up- or downregulated in transformed tissues, presumably to allow the tumor to evade the immune response.[24,25] It is highly possible that all these effects reflect altered antigenic repertoire profiles generated by these two aminopeptidases. However, a significant amount of information regarding the specificity and molecular properties of these enzymes is needed to understand these effects at the molecular and atomic levels.

Three recently determined structures of ERAP1 have yielded important insights into the molecular mechanism of the enzyme that makes it so appropriate for trimming antigenic peptide precursors.[12,26] These structures fall into two distinct categories depending on the relative orientation of domains II and IV of the enzyme. In the closed form, a very large internal cavity extending away from the catalytic site is occluded from access to the external solvent. In the open form, this cavity is exposed to the solvent and presumably facilitates the capture and binding of large peptide substrates. Even in the closed form, the internal cavity can accommodate the largest of antigenic peptide precursors and provide atomic interactions that determine specificity throughout the peptide sequence, influencing antigenic peptide selection. It has been hypothesized that long peptides can concurrently occupy the catalytic site and a distinct regulatory site and that this interaction leads to conformational rearrangements, enzyme activation, and efficient trimming.[12]

To improve our understanding of the exact role and molecular mechanism of ERAP2 in antigenic precursor processing, we crystallized human ERAP2 expressed from insect cells after baculovirus infection and determined the structure to a resolution of 3.08 Å. ERAP2 crystallizes as a homodimer through head-to-head interactions of the N-terminal domain that map an extended dimerization interface. Each monomer has an overall domain organization (domains I−IV) similar to that of the closed structure of ERAP1 [Protein Data Bank (PDB) entry 2YD0] with domain IV coming into the proximity of domain II, the catalytic site, and the S1 pocket (the latter defined as the specificity pocket accommodating the peptide side chain N-terminal to the scissile bond, according to the usual convention of defining peptidase specificity sites; subsequent specificity sites will be named S1′, S2′, etc.). This domain configuration generates an internal cavity that is of sufficient size to accommodate large peptides, similar to ERAP1. The shape and electrostatic potential distribution in that cavity, however, are distinct from the latter, suggesting that ERAP2 may apply distinct selective pressures in the antigenic peptide repertoire. Our structure provides an atomic-level explanation of the importance of residue Asp198 in ERAP2 N-terminal specificity. Furthermore, our structure suggests that specificity differences between ERAP1 and ERAP2 may extend throughout the peptide-binding cavity. We map a common SNP of ERAP2 (rs2549782, N392K), which has been linked with predisposition to disease, to a location adjacent to the active site of the enzyme. The ERAP2 homodimer in our structure is stabilized by an extended interface mediated by residues largely conserved in ERAP1 and may therefore constitute a useful model of the ERAP1−ERAP2 interaction. Overall, our structure provides insights into how two homologous aminopeptidases have evolved to be able to cooperate to trim a very large variety of peptide sequences, a function fundamental to their biological role in antigen processing.

EXPERIMENTAL PROCEDURES

Protein Expression and Purification. Human recombinant ERAP2 was produced using a baculovirus-driven insect cell expression system as previously described.[16] The purification procedure was modified to optimize purity for protein crystallography. Briefly, the cell supernatant was harvested 4 days postinfection, and protein content was bound to Cibacron Blue 3GA Agarose (Sigma). The resin was washed with 10 mM sodium phosphate (pH 7.0), and bound proteins were eluted with 500 mM NaCl and 10 mM sodium phosphate (pH 7.0). The eluate was then immediately bound to Ni-NTA agarose. ERAP2 was eluted using a buffer containing 300 mM NaCl, 50 mM imidazole, and 50 mM sodium phosphate (pH 8.0) and subsequently concentrated using a 10000 molecular weight cutoff filter (Sartorius). The enzyme was further purified by size-exclusion chromatography using a Sephadex S-200 column [pre-equilibrated with 150 mM NaCl, 0.01% NaN_3, and 25 mM HEPES (pH 7.0)] (Figure S1 of the Supporting Information). During purification, enzyme activity was followed by L-arginine-7-amido-4-methylcoumarin fluorigenic substrate hydrolysis.[27]

Crystallization. Crystals of ERAP2 were obtained from the Morpheus[28] protein crystallization screen (Molecular Dimensions Ltd.) using the sitting drop vapor diffusion technique. Crystals were obtained by mixing 200 nL of ERAP2 [6 mg/mL in 150 mM NaCl, 0.01% NaN_3, and 25 mM HEPES (pH 7.0)] with 100 nL of precipitant using an Oryx4 nanodrop crystallization robot (Douglas Instruments) and incubation with a 50 μL reservoir. Initial crystals appeared after 2−3 days under various Morpheus precipitant conditions at 10 °C and were optimized further by varying the protein:precipitant mixing ratios, the size of the drops, and the incubation temperature. The crystal used for data collection was grown in a 2 μL drop at 4 °C, using the following conditions: 10% PEG 8000; 20% ethylene glycol; glycine, DL-alanine, DL-serine, DL-lysine, and sodium glutamate (20 mM each); 31 mM MES; and 69 mM imidazole (pH 6.5).

Data Collection, Processing, and Refinement. High-resolution X-ray diffraction data were collected from a crystal frozen in a stream of N_2 gas at 100 K using synchrotron radiation (λ = 0.81230 Å) at beamline X13 (EMBL, Hamburg, Germany). Useful data were observed to 2.99 Å resolution. These were processed using the DENZO/SCALEPACK package.[29] Five percent of reflections were flagged for R_{free} calculations. The crystal belonged to space group $P2_1$ with the following cell dimensions: a = 74.6 Å, b = 134.4 Å, c = 128.0 Å, and β = 90.7° (Table 1). The unit cell is different from the unit cells of all the ERAP1 structures determined so far.

Table 1. Data Collection and Refinement Statistics of ERAP2

Data Collection	
space group	$P2_1$
a, b, c (Å)	74.6, 134.4, 128.0
β (deg)	90.7
resolution (Å)	19.5−3.08 (3.19−3.08)
R_{sym} (%)	8.4 (45.8)
$I/\sigma(I)$	11.6/2.0
completeness (%)	99.0 (99.1)
redundancy	2.8 (2.7)
Refinement	
resolution (Å)	11.0−3.08
no. of reflections (all/used)	43110/40931
R_{work}/R_{free} (%)	21.2/27.7 (28.7/40.2)[a]
no. of atoms (per asymmetric unit)	14348 (14 are alternate)
protein	14014
average B overall (Å^2)	66.4
NCS rmsd (Å)	
all atoms	0.44
D1 (55−271)	0.70
D2 (272−546)	0.39
D3 (547−637)	0.03
D4 (638−961)	0.28
rmsd for bond lengths (Å)	0.008
rmsd for bond angles (deg)	1.200
Ramachandran plot (%)	
preferred	88.9
allowed	9.1
outliers	2.0

[a]The outer shell for refinement is 3.13−3.08 Å. Values in parenthesis are for the outer shell.

The structure was determined by molecular replacement using MOLREP[30] using the "closed" ERAP1 structure (PDB entry 2XDT) as a search model. Two protein molecules, A and B, per asymmetric unit were found. REFMAC[31] was used for structure refinement by the maximum-likelihood method. Rigid body refinement was followed by several restrained refinement cycles. When an R factor of 25% had been reached, the refinement was continued with Phenix.refine[32] using data to 3.08 Å and imposing 2-fold NCS restraints. All residues, but 14 pairs of residues, were restrained according to NCS. Alternating cycles of restrained refinement with Phenix.refine and manual fitting and building with Coot[33] resulted in final R factor and R_{free} values of 21.2 and 27.7%, respectively. Refinement statistics are listed in Table 1. The Ramachandran plots as calculated with RAMPAGE[34] show that 88.9% of the residues lie in the preferred region, 9.1% in the allowed region, and 2% in the outlier region. The latter residues (34 overall, of which 28 are pairs of the same residues in the ERAP2 dimer) are located mainly in low-density loop regions at the exterior of the protein. Besides the two crystallographically independent protein molecules, the asymmetric unit comprises a total of 11 sugar residues and 126 water molecules. A lysine residue and a MES molecule were modeled on well-formed residual electron density close to the zinc ion of the active site of each protein molecule. The carbohydrate moieties were found attached to the following Asn N-glycosylation sites: A85, A219, A405, A650, B85, and B219. All occupancies of protein and carbohydrate atoms as well as water molecules were set to 1, except for those of the disordered amino acid side chains. Two amino acid side chains in one of the molecules (A) were disordered (Arg366 and Lys839) and refined with two alternative conformations. There was no assignable density before residue 54 of chain A and residue 55 of chain B. Also missing were residues 127−129, 503−527, and 570−580 of chain A and 126−132, 503−531, and 571−582 of chain B. All figures were made using PyMol (http://www.pymol.org).

RESULTS

Three-Dimensional Structure. The molecular structure of glycosylated human ERAP2 has been determined to 3.08 Å resolution by molecular replacement using ERAP1 (PDB entry 2XDT) as a search model and refined (Table 1 and Figure 1). The asymmetric unit contains two crystallographically independent ERAP2 molecules, A and B (Figure 1B), 126 water molecules, and 11 carbohydrate residues [a tetrasaccharide consisting of two *N*-acetylglucosamine (NAG) and two mannose (MAN) groups, two disaccharides of NAG, and

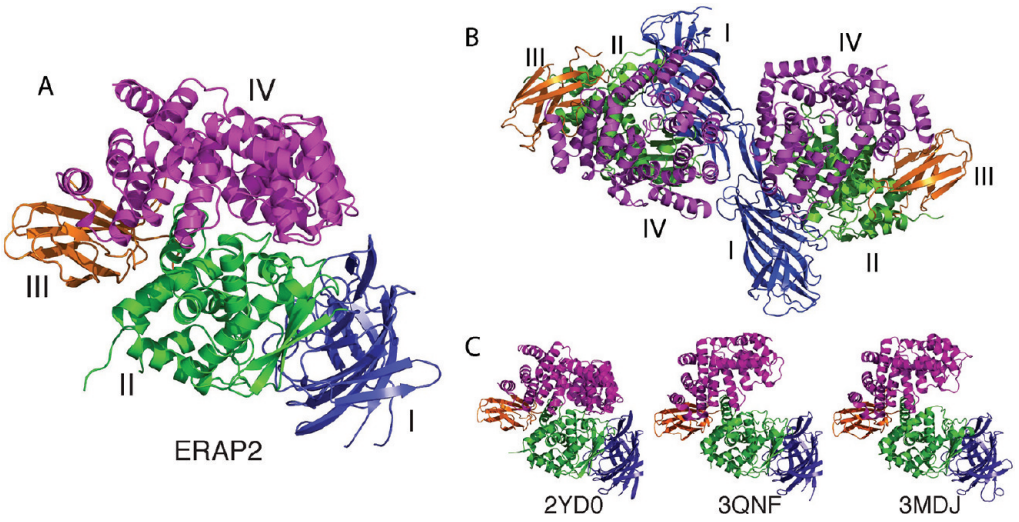

Figure 1. (A) Ribbon representation of the ERAP2 structure colored by domain (domains I in blue, II in green, III in orange, and IV in magenta). (B) Ribbon representation of the ERAP2 dimer in the asymmetric unit. Domains are colored as in panel A. (C) Ribbon representation of three ERAP1 structures (PDB entries 2YD0, 3QNF, and 3MDJ) aligned with the ERAP2 structure using domains I and II. Notice the differences in the relative positioning of domain IV.

dx.doi.org/10.1021/bi201230p | *Biochemistry* 2012, 51, 286−295

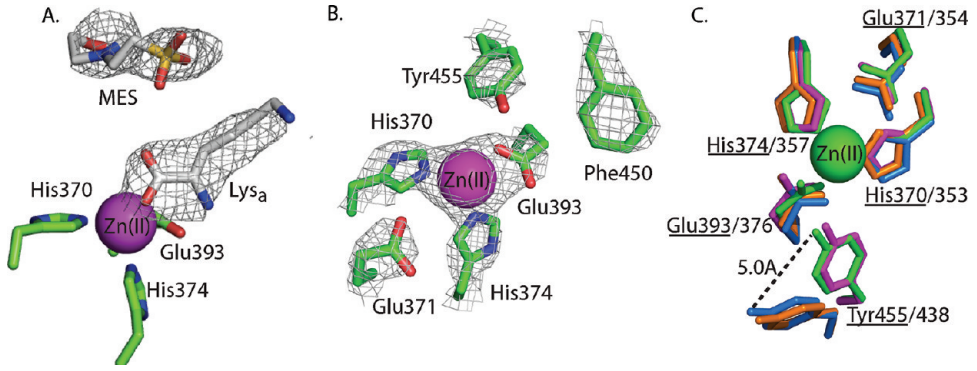

Figure 2. (A) Lysine (Lys$_a$) and MES ligands modeled into the active site based on residual difference ($|F_o| - |F_c|$) electron density (colored gray). (B) Detail of the catalytic site of ERAP2 showing the position and electron density ($2|F_o| - |F_c|$) of Zn(II) ion coordination and other key residues. (C) Relative positions of residues from the ERAP2 and ERAP1 catalytic sites. Notice how the positioning of Tyr455 and -438 differs between the open and closed forms of the enzymes. Residue numbers corresponding to ERAP2 are underlined.

three NAG monosaccharides]. All the carbohydrates are covalently bound to Asn side chains. The two ERAP2 molecules in the asymmetric unit are essentially identical, and during the final cycles of the refinement, noncrystallographic symmetry restraints (NCS) were applied.

Residual electron density (more than 3σ) was persistent in two locations close to the active site of both protein molecules A and B, after the end of the initial cycles of refinement (Figure 2A). Their elongated shape prompted us to model them as a molecule of L-lysine (Lys$_a$) coordinating the zinc and a molecule of 2-(*N*-morpholino)ethanesulfonic acid (MES), because both molecules were present at high concentrations in the crystallization mixture. L-Lysine was selected because positively charged amino acids are preferred by ERAP2, but another amino acid, i.e., glutamic acid, could also fit.

Each ERAP2 monomer is made of four structural domains (I–IV) forming a closed hollow structure (Figure 1A). The N-terminal domain I (residues 54–271) exhibits a β-sandwich structure. Domain II (residues 272–546) has a thermolysin α/β-fold and contains the HExxHx$_{18}$E zinc-binding motif as well as the GAMEN aminopeptidase motif. Domain III (residues 547–647) has a β-sandwich structure and acts as a link between domains II and IV. Domain IV (residues 648–960) is an all α-helical domain interacting closely with domain II, essentially capping the Zn(II) catalytic site. The contacts between domains II and IV define a large internal cavity, adjacent to the catalytic site, which has almost no access to the external solvent but exhibits numerous water molecules trapped inside it.

Overall, the ERAP2 domain organization resembles the recently determined structure of the "closed" conformation of the homologous aminopeptidase ERAP1 (PDB entry 2YD0) and is in contrast to two "open" forms of ERAP1 (also recently determined, PDB entries 3QNF and 3MDJ) showing domain IV moved away from domain II and exposing the internal cavity to the solvent (Figure 1C). Additionally, the ERAP2 domain organization resembles the structures of aminopeptidase N (PDB entry 2ZXG),[35,36] Tricorn interacting factor F3 (PDB entry 1Z5H),[37] and human leukotriene A4 hydrolase (PDB entries 1HS6 and 3B7U).[38,39] How these aminopeptidases relate structurally to ERAP1 and therefore to the highly similar ERAP2 has been discussed elsewhere.[26]

Catalytic Site. The catalytic site of ERAP2 features a single Zn(II) ion, coordinated by two histidine residues (H370 and H374) and glutamate residue E393 (the second Glu of the HExxHx$_{18}$E motif). The places of the fourth coordination sites of both Zn(II) ions of the dimer were occupied by the residual electron densities, which were modeled as lysine residues (Lys$_a$) (Figure 2A); thus, the carbonyl oxygen of C1 of Lys$_a$ is the fourth coordinating atom of the Zn(II) ion. Glu371 (the first Glu of the HExxHx$_{18}$E motif) is not in the first coordinating sphere of the zinc ion [4.2 Å (Figure 2B,C)] but is within H-bonding distance of the carbonyl group of Lys$_a$ (2.8 Å). The adjacent Phe450 lines the side of the S1 pocket of the enzyme, close to Lys$_a$ (shortest distance of 4.3 Å). A nearby tyrosine residue (Tyr455) is conserved in all M1 aminopeptidases and has been proposed to assist in the stabilization of the tetrahedral intermediate during the catalytic cycle.[35] This residue has been shown to be important for peptide hydrolysis by ERAP1 and to switch conformations depending on whether the enzyme is in the active or inactive form.[12] Comparison of the conformational state of Tyr455 in ERAP2 and the three known structures of ERAP1 (Figure 2C) indicates that ERAP2 in our structure is in the active closed form. The hydroxyl group of Tyr455 is located 3.0 Å from the second oxygen of the coordinating Lys$_a$.

S1 Pocket. The modeling of the Lys$_a$ residue in the active site helps identify the S1 pocket of the enzyme. The GAMEN motif, which is a fully conserved motif among all M1 aminopeptidases, is found adjacent to the catalytic site and is structurally identical to ERAP1. The GAMEN motif is considered to be responsible for recognizing the free N-terminus of the substrate and aligning the scissile bond in the appropriate position for nucleophilic attack (Figure 3A). The Gly334 and Ala335 residues of GAMEN, along with the adjacent Pro333, line the side of the specificity pocket, opposite Phe450. Glu337 of GAMEN forms a tight H-bond with the N-terminus of Lys$_a$ (2.7 Å). Glu337 is linked to the coordinating Glu393 through a water molecule, which forms H-bonds to the carboxylic side chains of both residues (distances of 2.4 and 2.6 Å, respectively), as well as to Glu200 (2.7 Å). The third side of the S1 pocket is lined by residues (Glu200 and Asp198) from domain I of the enzyme that provide interactions with Lys$_a$. The carboxylic group of Glu200 (Glu183 in ERAP1) forms a H-bond with the N-terminus of Lys$_a$ [2.9 Å (Figure 3A)]. Asp198 in ERAP2 has been shown to be critical for N-terminal specificity by site-directed mutagenesis as is the homologous Gln181 in ERAP1.[40] Asp198 forms a salt bridge (3.5 Å) with the side chain of Lys$_a$ (Figure 3B), an interaction that is possibly key to the S1 specificity of the enzyme.[16] The S1 pocket is capped by residues Glu177, Pro201, and Gln447 (His160, Pro184, and

dx.doi.org/10.1021/bi201230p | *Biochemistry* 2012, 51, 286–295

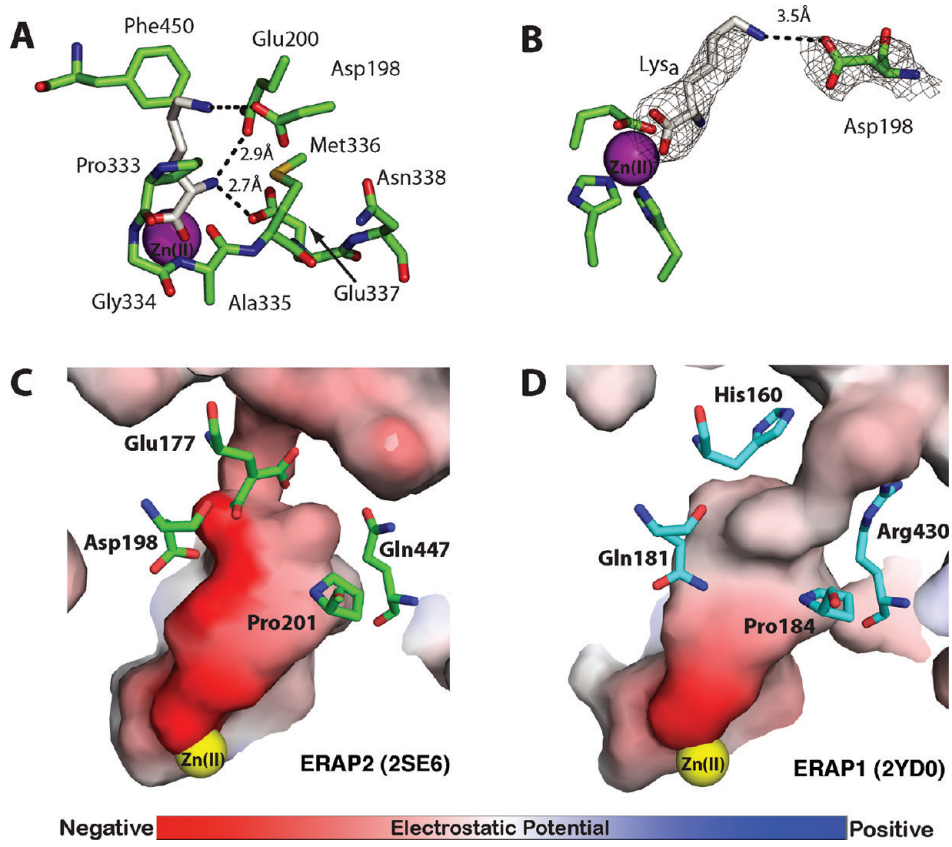

Figure 3. (A) Detail of the ERAP2 N-terminal recognition site and S1 pocket, showing the residues of the GAMEN motif as well as Asp198, which is important for N-terminal side chain preference. Active site ligand Lys_a is colored gray. (B) Interaction between Lys_a and Asp198 stabilizes the ligand side chain. The gray mesh around Lys_a corresponds to the difference electron density map ($|F_o| - |F_c|$). (C) ERAP2 and (D) ERAP1 catalytic and S1 specificity pocket in solvent accessible surface representation colored by electrostatic potential (red for negative and blue for positive). Residues that help form part of the pocket distal to the active site Zn(II) are shown as sticks. Notice the difference in electrostatic potential due primarily to the presence of two negatively charged residues (Asp198 and Glu177) in ERAP2.

Arg430 in ERAP1, respectively). These residue differences between ERAP1 and ERAP2 result in marked changes in the electrostatic potential of the base of the S1 pocket (Figure 3C,D), providing the molecular basis for the preference of ERAP2 for substrates with a positively charged N-terminal side chain.[16]

S1′ and Additional Pockets. The positioning of Lys_a as a model for the fourth coordinating group to the zinc ion provides clues about the location of the S1′ pocket. A putative, rather shallow pocket that could accommodate side chains from the second amino acid of a peptide substrate is lined by the zinc coordinating His370 and Glu371, Gly334 and Ala335 (of GAMEN), Trp363, and Val367. In the absence of a peptide substrate, this pocket is occupied partly by one conformer of disordered Arg366 and an H-bonding water molecule in this structure (distances of 3.0 Å to Arg366 and 3.5 Å to the noncoordinating oxygen of Lys_a).

The second residual electron density in the ERAP2 structure, close to the modeled Lys_a, has been modeled as a molecule of MES (31 mM under the crystallization conditions). The sulfonate sulfur atom is 3.2 Å from the second oxygen of Lys_a, thus close to where the second peptidic bond would be located. Its morpholino ring is situated between Tyr455 of domain II and Tyr892 of domain IV, which have their aromatic side chains oriented nearly parallel (Figure 4). The morpholino ring is actually entrapped between the two tyrosine residues (shortest distances of 3.9 and 3.4 Å, respectively) that form a

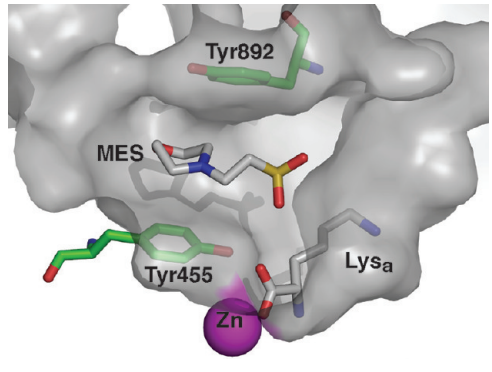

Figure 4. Postulated S′ specificity pocket in ERAP2. The MES ligand (gray) was found to be stabilized by stacking interactions with residues Tyr455 and Tyr892 (green sticks).

hydrophobic channel between domains II and IV. It is possible that this narrow channel constitutes a specificity pocket for the enzyme, which can accommodate aromatic side chains. In this structure, a long peptide substrate can be threaded through this channel to extend farther into the internal cavity. The remaining walls of the channel comprise the main chain of residues Phe450 and Asn451 on the third side and Ala396 and Lys397 on the fourth.

Internal Cavity. Beyond the channel mentioned above, the internal cavity expands throughout the whole interface of

dx.doi.org/10.1021/bi201230p | *Biochemistry* 2012, 51, 286−295

domains II and IV (starting from the interface of domain IV with III). This cavity has an overall excluded area (as calculated with GRASP[41]) of 3334 Å^2, which is comparable to the corresponding area of the cavity identified in the closed conformational state of ERAP1[26] (3185 Å^2); thus, it is sufficiently large that it can accommodate even large antigenic peptide precursors in a conformation that aligns their N-termini with the catalytic site. Interactions between specificity pockets in this cavity and side chains of the peptide substrate have been hypothesized to underlie substrate specificity for ERAP1.[12,14] Although not much different in size, the cavities of ERAP2 and ERAP1 display numerous differences in the side chains lining them and particularly in the side chains originating from the less homologous domain IV. Such changes may be sufficient in directing different substrate preferences between the two enzymes. Specifically, the number of ionizable side chains of the cavity surface differ in the two enzymes: ERAP2 exhibits 11 acidic and 6 basic side chains in domain II and 8 acidic and 11 basic side chains in domain IV, whereas ERAP1 has 13 acidic and 6 basic side chains in domain II and 6 acidic and 6 basic side chains in domain IV. Similarly, differences are observed in other polar residues (with hydroxylic or amide side chains) (17 in each in domains II and IV of ERAP2 but 12 and 25 for the respective domains of ERAP1), whereas the number of their nonpolar residues is comparable. Therefore, the presence of shallow or deep pockets that could operate as specificity pockets and the distribution of electrostatic potential in the cavity are distinct for the two enzymes (Figure 5). The negative electrostatic potential in the ERAP1 internal cavity has been suggested to be responsible for selectivity for substrates that carry positively charged side chains.[12,14] The different electrostatic potential distribution in the cavity of ERAP2 (more positively charged side groups) suggests that the enzyme may have different preferences for substrate sequence compared to ERAP1, something consistent with a distinct and/or complementary role in antigen processing.[15]

The preference of ERAP1 to trim larger substrates but spare shorter ones has led to the proposal of a "molecular ruler" mechanism.[11] It has been suggested that this property may stem from the recognition of the C-terminus of the peptide by a deep pocket inside the cavity of ERAP1 which is at a sufficient distance from the catalytic site that it can be occupied concurrently by only long peptides.[26] Although two of the three residues that help form this pocket in ERAP1 (Phe882 and Arg841) are conserved in ERAP2 (Phe905 and Arg864), the pocket is not formed in the latter (Figure 6), possibly because of the positioning of His904 in ERAP2 (Gln881 in ERAP1). This finding may underlie the different length preferences that ERAP2 has been suggested to have.[11]

Homodimer. ERAP2 was found to crystallize as a homodimer in the asymmetric unit. Dimerization is mediated mainly by interactions of domain I of monomers A and B, in a head-to-head fashion (Figure 1B), which define an excluded area of 1147 Å^2 (calculated by GRASP; 986 Å^2 between the domains I of each monomer and 161 Å^2 between domains IV of each monomer). Several residues participate in this interaction, and most of them are conserved in ERAP1 (Table 2). In the middle of the interaction area, a portion of β-strand 9 of domain I of each monomer interact in a β-sheet-like configuration so that β-strands 8 and 9 from each monomer form a four-stranded antiparallel β-sheet structure between the domains. Specifically, the main chains of Thr191 form mutual hydrogen bonds between their carbonyl oxygen and amide nitrogen atoms (2.9 and 3.0 Å). The lack of further main chain interactions is compensated by side chain ion pairs, Glu190 of molecule B to Arg229 of molecule A (2.8 Å) and vice versa, Glu190 of molecule A to Arg229 of molecule B (3.2 Å), and the nonconventional H-bond from H(CD1) of Ile193 to the carbonyl oxygen atom of Gly188 of both monomers (C-C distances 3.3 and 3.0 Å for molecules A and B, respectively). At the outer part, Thr87 interacts with Asp291 and Leu86-Thr87-Ser88-Leu89 loops of each monomer come close to the corresponding Leu187-Gly188 loops. Interestingly, the residues listed in the interactions mentioned above are conserved in ERAP1 and ERAP2 (in bold in Table 2). Finally, two strong ion pair interactions between domain IV residues Glu813 and Lys848 of monomers A and B (2.6 and 2.9 Å, respectively) are observed.

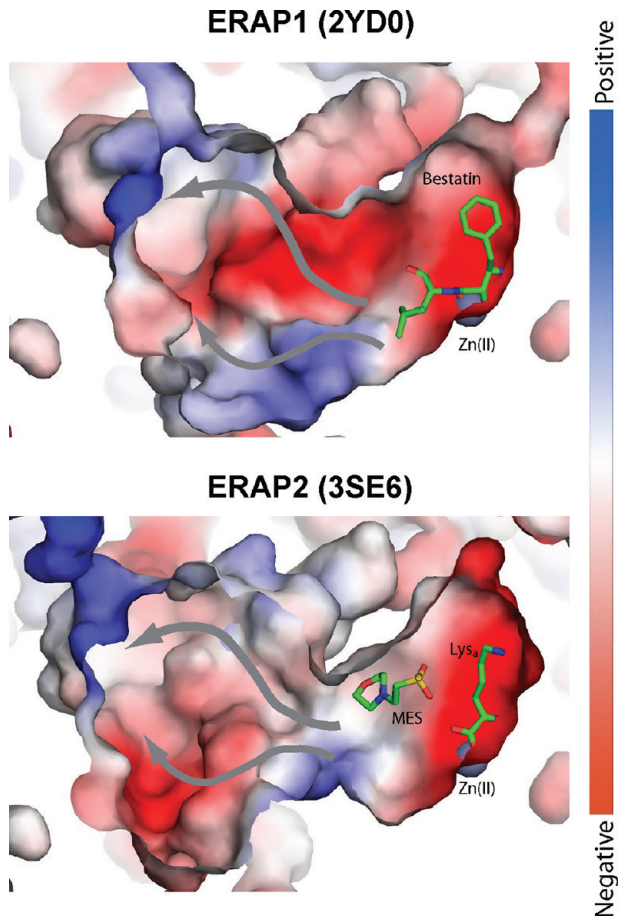

Figure 5. ERAP1 (top) and ERAP2 (bottom) internal cavities in surface representation, colored by electrostatic potential. Active site ligands (bestatin for ERAP1 and Lys$_a$ and MES for ERAP2) are shown as sticks, and Zn(II) is shown as a gray sphere. Gray arrows show possible binding configurations for a peptide substrate.

Interestingly, the most ordered carbohydrate chains (a tetrasaccharide and a disaccharide), originating from residue Asn85 of monomers B and A, respectively, contribute also in the stabilization of the contact region between domain I of the A and B ERAP2 monomers (Figure S3 of the Supporting Information). The first NAG residues of each ERAP2 monomer are stabilized by H-bonds between their *N*-acetyl groups and the His83 NE2 atoms of the monomers from which they originate whereas the second NAG residues by H-bonds between the *N*-acetyl groups and His272 of the opposite protein in the dimer. An additional H-bond is formed between the guanidine group of Arg293 of ERAP2 monomer

dx.doi.org/10.1021/bi201230p | *Biochemistry* 2012, 51, 286−295

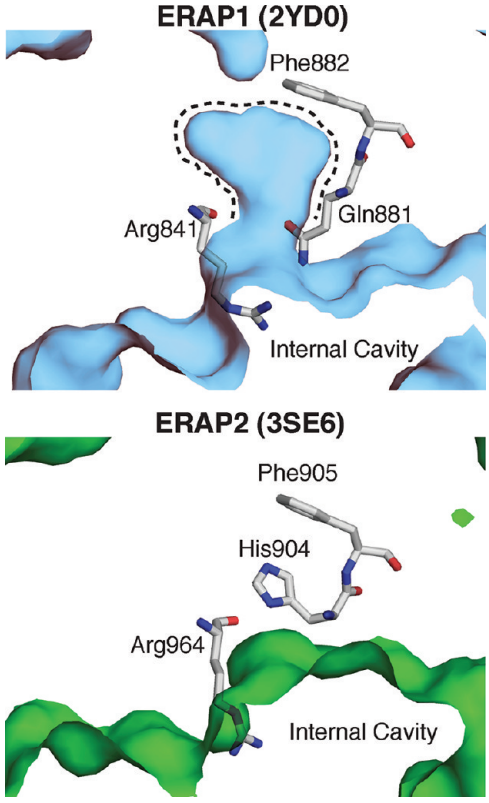

Figure 6. Detail of the internal cavity of ERAP1 (top, cyan) and ERAP2 (bottom, green) showing the location of the hypothesized C-terminal recognition pocket in ERAP1 (dashed line) and the equivalent location in ERAP2. Residues of ERAP1 (and homologous residues in ERAP2) that define the pocket are shown as sticks. Notice the apparent absence of such a pocket for ERAP2. The view slab was set at 5 Å.

Table 2. Residues Lining the Interacting ERAP2 Monomer Surfaces (as determined by GRASP) or Interact with the Carbohydrate Chains

ERAP2 chain A	ERAP2 chain B	ERAP1 homologous amino acid
Asn85	**Asn85**	**Asn70**
Leu86	**Leu86**	**Leu71**
Thr87	**Thr87**	**Thr72**
	Ser88	**Thr73**
Leu89	**Leu89**	**Leu74**
Thr183	**Thr183**	**Thr166**
Leu187	Leu187	Lys170
Gly188	Gly188	Glu171
Gly189	**Gly189**	**Gly172**
Glu190	**Glu190**	**Glu173**
Thr191	Thr191	Leu174
Arg192	**Arg192**	**Arg175**
Ile193	**Ile193**	**Ile176**
Arg229	**Arg229**	**Arg212**
His272	His272	Glu255
Asp291	**Asp291**	**Asp274**
Arg293	Arg293	Ile276
Glu813	Glu813	Gln790
Glu846	Glu846	Lys823
Lys848	Lys848	Asp825
Val849	Val849	Lys826

A and the carbohydrate oligomer originating from monomer B (O2 of mannose 1). A similarly sized carbohydrate chain was found in a crystal structure of ERAP1 (PDB entry 3MDJ), but in that case, it does not participate in any intermolecular interactions.

DISCUSSION

ERAP2 Is in an Active Form with a Product Trapped in the Active Site. In this study, we determined the three-dimensional structure of human ERAP2 to 3.08 Å resolution by X-ray crystallography. ERAP2 has been suggested to act as an accessory aminopeptidase to ERAP1, assisting in trimming residues and sequences that ERAP1 trims poorly. The two aminopeptidases are highly homologous (~49% average sequence identity, but individually 58, 60, 47, and 43% for domains I–IV, respectively) and have the same domain organization. ERAP2 was found to be in a closed conformation in which domain IV interacts with an extended part of domain II, resulting in a large internal cavity that is not accessible to the external solvent but in which several water molecules are entrapped. The cavity, similar to the cavity in ERAP1, extends from the Zn(II) catalytic site of the enzyme and may accommodate large peptide substrates consistent with the proposed biological role of ERAP2 in trimming long peptide substrates, precursors to antigenic epitopes. The fact that the cavity has no direct access to the external solvent suggests that the enzyme has to undergo changes in conformation to allow substrate approach and product release as in ERAP1. The lysine residue, Lys_a, that was modeled as the fourth coordinating ligand of the Zn ion is positioned in a configuration that would be expected to resemble the binding of the N-terminal amino acid of a peptide substrate. The orientation of Tyr455 suggests that the enzyme is in the active configuration. Overall, our structure corresponds to the enzyme–product complex, the product being the released amino-terminal amino acid, which is still trapped in the active site until conformational rearrangements of the enzyme allow it to diffuse away in preparation for the next catalytic cycle.

Structural Determinants Support Distinct Specificity. Further comparison of the ERAP2 structure with the closed ERAP1 structure yields insight into their distinct biological roles. Although the two structures are highly similar with rmsds of 1.36 Å for main chain atoms and 1.52 Å for all atoms (rmsds for all atoms of 1.27 Å for domain I, 0.99 Å for domain II, 1.24 Å for domain III, and 1.60 Å for domain IV), key differences can affect antigen processing by altering the specificity of substrate recognition. This is clear with regard to the S1 specificity, where a key change at Gln181 in ERAP1 to Asp198 in ERAP2 and changes in residues capping the pocket (His160 and Arg430 in ERAP1 to Glu177 and Gln447 in ERAP2) result in marked differences in the electrostatic potential of the S1 pocket. We therefore provide an atomic-level explanation for the different S1 specificity between the two enzymes. This specificity change is potentially crucial for their biological role, because it allows ERAP2 to trim N-terminal amino acids for which ERAP1 has reduced activity.

Inspection of the internal cavity that extends away from the active site and comparison to the equivalent cavity of ERAP1 suggest that although the two enzymes may have a common substrate recognition mechanism, the S′ specificity pockets of each enzyme may be significantly different. Peptide sequence specificities have previously been demonstrated experimentally for ERAP1, suggesting the presence of at least some S′ specificity sites.[14] Although the unequivocal definition of such pockets is speculative in the absence of structural information about an enzyme–substrate complex, differences between possible interaction sites in ERAP1 and ERAP2 are sufficiently frequent

to support different specificities for peptide sequence. Analysis of the overall electrostatic potential of the cavity in ERAP1 and ERAP2 reveals distinct patterns that may affect substrate preferences. The strongly negative electrostatic potential in ERAP1 has been linked with a preference for substrates carrying one or more positively charged amino acids in their sequence. The different distribution of electrostatic potential in ERAP2 may suggest that this preference may not be shared by ERAP2, at least not for the same positions. This property may allow ERAP2 to extend its complementarity in substrate preference farther from just the S1 pocket to the whole peptide sequence. It is reasonable therefore to hypothesize that sequence-specific selectivity pressures in the antigenic peptide repertoire of ERAP1[8,10] may be extended or in some cases even ameliorated by the different specificity of ERAP2. This may be a key difference in antigen processing between humans and mice because the latter do not have the gene for ERAP2.

The ERAP2 Homodimer as a Model for the ERAP1−ERAP2 Interaction. Although ERAP2 crystallized as a homodimer, size-exclusion chromatography analysis and dynamic light scattering analysis suggested that it is predominantly a monomer in solution at concentrations of <1 mg/mL (Figure S1 of the Supporting Information). However, we cannot rule out the possibility that ERAP2 homodimerizes inside the limited space of the ER where local concentrations can be much higher (as they are during crystallization). Additionally, a homodimer for the highly homologous IRAP has been recently demonstrated and proposed to have a topology similar to that of the ERAP2 homodimer.[42] Furthermore, ERAP2 has been proposed to function in concert with ERAP1 by forming a heterodimer.[15] Although the exact nature of this dimer is still speculative, the ERAP2 homodimer found in the asymmetric unit has key features that may make it an appropriate model for the ERAP1−ERAP2 interaction. First, the extent of the excluded surface area between the monomers has been suggested to indicate that the interaction may be specific (<5% probability that the proposed dimer is not functionally relevant according to the analysis as presented in ref 43). Second, the ERAP2 homodimer interaction is mainly through the conserved N-terminal domain I and is mediated by conserved amino acid residues and highly ordered carbohydrates, which are also present in ERAP1. Interestingly, it has been recently shown that carbohydrate structures are necessary for the function of the peptide loading complex (PLC) in which ERAP1 is believed to participate.[44] Furthermore, the dimer topology is such that it allows for access of the peptide to the active site and the necessary domain motions involving domain IV. The hinge region domain III does not participate in dimer contacts, thereby not hindering possible conformational changes during catalysis. Finally, the relative orientation of the two chains puts the two catalytic sites facing each other, a configuration that may facilitate exchange of substrates during catalytic cycles as proposed for long peptide substrates.[15] On the basis of this dimerization of our structure, it is possible to create a hypothetical model of the ERAP1−ERAP2 dimer in different catalytic cycles (Figure S4 of the Supporting Information).

Mapping a Disease-Linked Single-Nucleotide Polymorphism. The N392K single-nucleotide polymorphism in ERAP2 (rs2549782) has been linked with a predisposition to several human diseases, possibly through the role of ERAP2 in antigen processing and generation.[17,20−23,45] The crystal structure of ERAP2 described here allows for the first time the accurate mapping of the location of this important polymorphism (Figure S5 of the Supporting Information). In this structure, Asn392 is very close to the enzyme's catalytic site and specifically to several catalytically important residues, such as Glu200, Glu337, and Glu393. Furthermore, Asn392 makes atomic interactions with nearby residues, most notably with Tyr262 (3.1 Å). As a result, the N392K mutation would be expected to perturb the local structure in ERAP2, because of the longer size of the lysine residue or its charge. Such perturbations in the proximity to the catalytic site of the enzyme could affect the catalytic efficiency and the antigen processing properties of the enzyme. Indeed, preliminary analysis suggests that this replacement can affect the catalytic turnover of the enzyme (E. Stratikos et al., unpublished results to be presented elsewhere).

In summary, we describe the first crystal structure of human ERAP2, an important enzyme in the functioning of antigen presentation and the adaptive immune response. The ERAP2 structure resembles the closed active form of the homologous and recently crystallized ERAP1 but features key differences in the peptide-binding internal cavity that are consistent with a distinct or complementary role in antigen processing. Our structure lays the groundwork for understanding why three separate aminopeptidases are required by the cell for what initially appeared to be a simple trimming process but has evolved to become a novel paradigm in immune response regulation. Furthermore, the ERAP2 structure will undoubtedly be useful for the rational design and evaluation of selective inhibitors that can modulate antigen processing and the adaptive immune response.

■ ASSOCIATED CONTENT

Supporting Information

Additional methods and data. This material is available free of charge via the Internet at http://pubs.acs.org.

Accession Codes

Atomic coordinates and structure factors have been deposited in the Protein Data Bank as entry 3SE6.

■ AUTHOR INFORMATION

Corresponding Author

*I.M.M.: Structural and Supramolecular Chemistry Laboratory, Institute of Physical Chemistry, National Center for Scientific Research Demokritos, Aghia Paraskevi 15310, Athens, Greece; e-mail, mavridi@chem.demokritos.gr; telephone, +302106503793. E. Stratikos: Protein Chemistry Laboratory, IRRP, National Center for Scientific Research Demokritos, Aghia Paraskevi 15310, Athens, Greece; e-mail, stratos@rrp.demokritos.gr; telephone, +302106503918.

Funding

This work was funded by European Commission Grant FP7-Marie Curie-IAPP-TOPCRYST (217979). Partial funding from EMBL (Hamburg, Germany; Grant HPMT-CT-2000-00174) and by a grant from the Hellenic Rheumatology Society (E. Stratikos) is gratefully acknowledged.

■ ACKNOWLEDGMENTS

We thank Ms. Irini Evnouchidou for help with the construction of the recombinant baculovirus and for helpful discussions and Dr. Petros Giastas for generous assistance with the crystallization. We are also grateful to Dr. Matthew Groves and Dr. Spyros Chatziefthimiou (EMBL) for their assistance.

■ ABBREVIATIONS

ER, endoplasmic reticulum; ERAP1 and ERAP2, endoplasmic reticulum aminopeptidases 1 and 2, respectively; PLC, peptide loading complex; SNP, single-nucleotide polymorphism; MHCI, major histocompatibility complex class I; rmsd, root-mean-square deviation; S1 pocket, first specificity pocket according to the standard convention of protease specificity; S1′, S2′, etc., specificity pockets recognizing side chains C-terminal to the scissile bond.

■ REFERENCES

(1) Rock, K. L., and Goldberg, A. L. (1999) Degradation of cell proteins and the generation of MHC class I-presented peptides. *Annu. Rev. Immunol. 17*, 739−779.

(2) Rock, K. L. (2006) Exiting the outside world for cross-presentation. *Immunity 25*, 523−525.

(3) Cascio, P., Hilton, C., Kisselev, A. F., Rock, K. L., and Goldberg, A. L. (2001) 26S proteasomes and immunoproteasomes produce mainly N-extended versions of an antigenic peptide. *EMBO J. 20*, 2357−2366.

(4) Serwold, T., Gaw, S., and Shastri, N. (2001) ER aminopeptidases generate a unique pool of peptides for MHC class I molecules. *Nat. Immunol. 2*, 644−651.

(5) Evnouchidou, I., Papakyriakou, A., and Stratikos, E. (2009) A New Role for Zn(II) Aminopeptidases: Antigenic Peptide Generation and Destruction. *Curr. Pharm. Des. 15*, 3656−3670.

(6) York, I. A., Chang, S. C., Saric, T., Keys, J. A., Favreau, J. M., Goldberg, A. L., and Rock, K. L. (2002) The ER aminopeptidase ERAP1 enhances or limits antigen presentation by trimming epitopes to 8−9 residues. *Nat. Immunol. 3*, 1177−1184.

(7) Serwold, T., Gonzalez, F., Kim, J., Jacob, R., and Shastri, N. (2002) ERAAP customizes peptides for MHC class I molecules in the endoplasmic reticulum. *Nature 419*, 480−483.

(8) York, I. A., Brehm, M. A., Zendzian, S., Towne, C. F., and Rock, K. L. (2006) Endoplasmic reticulum aminopeptidase 1 (ERAP1) trims MHC class I-presented peptides in vivo and plays an important role in immunodominance. *Proc. Natl. Acad. Sci. U.S.A. 103*, 9202−9207.

(9) Hammer, G. E., Gonzalez, F., Champsaur, M., Cado, D., and Shastri, N. (2006) The aminopeptidase ERAAP shapes the peptide repertoire displayed by major histocompatibility complex class I molecules. *Nat. Immunol. 7*, 103−112.

(10) Hammer, G. E., Gonzalez, F., James, E., Nolla, H., and Shastri, N. (2007) In the absence of aminopeptidase ERAAP, MHC class I molecules present many unstable and highly immunogenic peptides. *Nat. Immunol. 8*, 101−108.

(11) Chang, S. C., Momburg, F., Bhutani, N., and Goldberg, A. L. (2005) The ER aminopeptidase, ERAP1, trims precursors to lengths of MHC class I peptides by a "molecular ruler" mechanism. *Proc. Natl. Acad. Sci. U.S.A. 102*, 17107−17112.

(12) Nguyen, T. T., Chang, S. C., Evnouchidou, I., York, I. A., Zikos, C., Rock, K. L., Goldberg, A. L., Stratikos, E., and Stern, L. J. (2011) Structural basis for antigenic peptide precursor processing by the endoplasmic reticulum aminopeptidase ERAP1. *Nat. Struct. Mol. Biol. 18*, 604−613.

(13) Georgiadou, D., and Stratikos, E. (2009) Cellular mechanisms that edit the immunopeptidome. *Curr. Proteomics 6*, 13−24.

(14) Evnouchidou, I., Momburg, F., Papakyriakou, A., Chroni, A., Leondiadis, L., Chang, S. C., Goldberg, A. L., and Stratikos, E. (2008) The internal sequence of the peptide-substrate determines its N-terminus trimming by ERAP1. *PLoS One 3*, e3658.

(15) Saveanu, L., Carroll, O., Lindo, V., Del Val, M., Lopez, D., Lepelletier, Y., Greer, F., Schomburg, L., Fruci, D., Niedermann, G., and van Endert, P. M. (2005) Concerted peptide trimming by human ERAP1 and ERAP2 aminopeptidase complexes in the endoplasmic reticulum. *Nat. Immunol. 6*, 689−697.

(16) Zervoudi, E., Papakyriakou, A., Georgiadou, D., Evnouchidou, I., Gajda, A., Poreba, M., Salvesen, G. S., Drag, M., Hattori, A., Swevers, L., Vourloumis, D., and Stratikos, E. (2011) Probing the S1 specificity pocket of the aminopeptidases that generate antigenic peptides. *Biochem. J. 435*, 411−420.

(17) Haroon, N., and Inman, R. D. (2010) Endoplasmic reticulum aminopeptidases: Biology and pathogenic potential. *Nat. Rev. Rheumatol. 6*, 461−467.

(18) Tsui, F. W., Haroon, N., Reveille, J. D., Rahman, P., Chiu, B., Tsui, H. W., and Inman, R. D. (2010) Association of an ERAP1 ERAP2 haplotype with familial ankylosing spondylitis. *Ann. Rheum. Dis. 69*, 733−736.

(19) Evnouchidou, I., Kamal, R. P., Seregin, S. S., Goto, Y., Tsujimoto, M., Hattori, A., Voulgari, P. V., Drosos, A. A., Amalfitano, A., York, I. A., and Stratikos, E. (2011) Coding single nucleotide polymorphisms of endoplasmic reticulum aminopeptidase 1 can affect antigenic peptide generation in vitro by influencing basic enzymatic properties of the enzyme. *J. Immunol. 186*, 1909−1913.

(20) Cagliani, R., Riva, S., Biasin, M., Fumagalli, M., Pozzoli, U., Lo Caputo, S., Mazzotta, F., Piacentini, L., Bresolin, N., Clerici, M., and Sironi, M. (2010) Genetic diversity at endoplasmic reticulum aminopeptidases is maintained by balancing selection and is associated with natural resistance to HIV-1 infection. *Hum. Mol. Genet. 19*, 4705−4714.

(21) Andres, A. M., Dennis, M. Y., Kretzschmar, W. W., Cannons, J. L., Lee-Lin, S. Q., Hurle, B., Program, N. C. S., Schwartzberg, P. L., Williamson, S. H., Bustamante, C. D., Nielsen, R., Clark, A. G., and Green, E. D. (2010) Balancing selection maintains a form of ERAP2 that undergoes nonsense-mediated decay and affects antigen presentation. *PLoS Genet. 6*, e1001157.

(22) Tenzer, S., Wee, E., Burgevin, A., Stewart-Jones, G., Friis, L., Lamberth, K., Chang, C. H., Harndahl, M., Weimershaus, M., Gerstoft, J., Akkad, N., Klenerman, P., Fugger, L., Jones, E. Y., McMichael, A. J., Buus, S., Schild, H., van Endert, P., and Iversen, A. K. (2009) Antigen processing influences HIV-specific cytotoxic T lymphocyte immunodominance. *Nat. Immunol. 10*, 636−646.

(23) Johnson, M. P., Roten, L. T., Dyer, T. D., East, C. E., Forsmo, S., Blangero, J., Brennecke, S. P., Austgulen, R., and Moses, E. K. (2009) The ERAP2 gene is associated with preeclampsia in Australian and Norwegian populations. *Hum. Genet. 126*, 655−666.

(24) Fruci, D., Ferracuti, S., Limongi, M. Z., Cunsolo, V., Giorda, E., Fraioli, R., Sibilio, L., Carroll, O., Hattori, A., van Endert, P. M., and Giacomini, P. (2006) Expression of endoplasmic reticulum aminopeptidases in EBV-B cell lines from healthy donors and in leukemia/lymphoma, carcinoma, and melanoma cell lines. *J. Immunol. 176*, 4869−4879.

(25) Fruci, D., Giacomini, P., Nicotra, M. R., Forloni, M., Fraioli, R., Saveanu, L., van Endert, P., and Natali, P. G. (2008) Altered expression of endoplasmic reticulum aminopeptidases ERAP1 and ERAP2 in transformed non-lymphoid human tissues. *J. Cell. Physiol. 216*, 742−749.

(26) Kochan, G., Krojer, T., Harvey, D., Fischer, R., Chen, L., Vollmar, M., von Delft, F., Kavanagh, K. L., Brown, M. A., Bowness, P., Wordsworth, P., Kessler, B. M., and Oppermann, U. (2011) Crystal structures of the endoplasmic reticulum aminopeptidase-1 (ERAP1) reveal the molecular basis for N-terminal peptide trimming. *Proc. Natl. Acad. Sci. U.S.A. 108*, 7745−7750.

(27) Evnouchidou, I., Berardi, M. J., and Stratikos, E. (2009) A continuous fluorigenic assay for the measurement of the activity of endoplasmic reticulum aminopeptidase 1: Competition kinetics as a tool for enzyme specificity investigation. *Anal. Biochem. 395*, 33−40.

(28) Gorrec, F. (2009) The MORPHEUS protein crystallization screen. *J. Appl. Crystallogr. 42*, 1035−1042.

(29) Otwinowski, Z., and Minor, W. (1997) Processing of X-ray diffraction data collected in oscillation mode. *Methods Enzymol. 276*, 307−326.

(30) Vagin, A., and Teplyakov, A. (2010) Molecular replacement with MOLREP. *Acta Crystallogr. D66*, 22−25.

(31) Murshudov, G. N., Vagin, A. A., and Dodson, E. J. (1997) Refinement of macromolecular structures by the maximum-likelihood method. *Acta Crystallogr. D53*, 240−255.

(32) Adams, P. D., Afonine, P. V., Bunkoczi, G., Chen, V. B., Davis, I. W., Echols, N., Headd, J. J., Hung, L. W., Kapral, G. J., Grosse-Kunstleve, R. W., McCoy, A. J., Moriarty, N. W., Oeffner, R., Read, R. J., Richardson, D. C., Richardson, J. S., Terwilliger, T. C., and Zwart, P. H. (2010) PHENIX: A comprehensive Python-based system for macromolecular structure solution. *Acta Crystallogr. D66*, 213−221.
(33) Emsley, P., and Cowtan, K. (2004) Coot: Model-building tools for molecular graphics. *Acta Crystallogr. D60*, 2126−2132.
(34) Lovell, S. C., Davis, I. W., Arendall, W. B. III, de Bakker, P. I., Word, J. M., Prisant, M. G., Richardson, J. S., and Richardson, D. C. (2003) Structure validation by Cα geometry: ϕ, ψ and Cβ deviation. *Proteins 50*, 437−450.
(35) Addlagatta, A., Gay, L., and Matthews, B. W. (2006) Structure of aminopeptidase N from *Escherichia coli* suggests a compartmentalized, gated active site. *Proc. Natl. Acad. Sci. U.S.A. 103*, 13339−13344.
(36) Addlagatta, A., Gay, L., and Matthews, B. W. (2008) Structural basis for the unusual specificity of *Escherichia coli* aminopeptidase N. *Biochemistry 47*, 5303−5311.
(37) Kyrieleis, O. J., Goettig, P., Kiefersauer, R., Huber, R., and Brandstetter, H. (2005) Crystal structures of the tricorn interacting factor F3 from *Thermoplasma acidophilum*, a zinc aminopeptidase in three different conformations. *J. Mol. Biol. 349*, 787−800.
(38) Thunnissen, M. M., Nordlund, P., and Haeggstrom, J. Z. (2001) Crystal structure of human leukotriene A_4 hydrolase, a bifunctional enzyme in inflammation. *Nat. Struct. Biol. 8*, 131−135.
(39) Tholander, F., Muroya, A., Roques, B. P., Fournie-Zaluski, M. C., Thunnissen, M. M., and Haeggstrom, J. Z. (2008) Structure-based dissection of the active site chemistry of leukotriene A4 hydrolase: Implications for M1 aminopeptidases and inhibitor design. *Chem. Biol. 15*, 920−929.
(40) Goto, Y., Tanji, H., Hattori, A., and Tsujimoto, M. (2008) Glutamine-181 is crucial in the enzymatic activity and substrate specificity of human endoplasmic-reticulum aminopeptidase-1. *Biochem. J. 416*, 109−116.
(41) Nicholls, A., Sharp, K. A., and Honig, B. (1991) Protein folding and association: Insights from the interfacial and thermodynamic properties of hydrocarbons. *Proteins 11*, 281−296.
(42) Ascher, D. B., Cromer, B. A., Morton, C. J., Volitakis, I., Cherny, R. A., Albiston, A. L., Chai, S. Y., and Parker, M. W. (2011) Regulation of Insulin-Regulated Membrane Aminopeptidase Activity by Its C-terminal Domain. *Biochemistry 50*, 2611−2622.
(43) Janin, J. (1997) Specific versus non-specific contacts in protein crystals. *Nat. Struct. Biol. 4*, 973−974.
(44) Wearsch, P. A., Peaper, D. R., and Cresswell, P. (2011) Essential glycan-dependent interactions optimize MHC class I peptide loading. *Proc. Natl. Acad. Sci. U.S.A. 108*, 4950−4955.
(45) Tsui, F. W., Haroon, N., Reveille, J. D., Rahman, P., Chiu, B., Tsui, H. W., and Inman, R. D. (2010) Association of an ERAP1 ERAP2 haplotype with familial ankylosing spondylitis. *Ann. Rheum. Dis. 69*, 733−736.